12-10-1998

Tertiary remagnetization of Paleozoic rocks from the Eastern Cordillera and sub-Andean Belt of Bolivia

J. C. Libarkin

Robert F. Butler
University of Portland, butler@up.edu

D. R. Richards

T. Sempere

JOURNAL OF GEOPHYSICAL RESEARCH, VOL. 103, NO. B12, PAGES 30,417–30,429, DECEMBER 10, 1998

Tertiary remagnetization of Paleozoic rocks from the Eastern Cordillera and sub-Andean Belt of Bolivia

J. C. Libarkin, R. F. Butler, and D. R. Richards
Department of Geosciences, University of Arizona, Tucson

T. Sempere
Misión Orstom en el Perú, Lima

Abstract. Paleomagnetic samples were collected from 98 sedimentary horizons in eight different Devonian to Permian sedimentary units at eight localities in the Eastern Cordillera and the sub-Andean Belt of Bolivia. For 77 sites, thermal demagnetization allowed determination of a characteristic magnetization (ChRM) with site-mean 95% confidence limit, α_{95}, $\leq 15°$. The ChRM is carried predominantly or entirely by hematite. Fold and reversal tests from two of the sampled localities indicate that the characteristic magnetization is synfolding, likely acquired during the earliest stages of deformation. Additionally, a modified conglomerate test at one locality and the nearly uniform direction of ChRM across the Devonian to Permian age units clearly reveals the secondary nature of the characteristic magnetization. Finally, the ChRM directions are discordant from any expected Paleozoic directions. Paleomagnetic poles calculated from the ChRM directions fall near the Cenozoic portion of the apparent polar wander path for South America. We interpret these observations to indicate widespread chemical remagnetization of these Paleozoic strata during, but prior to completion of, Cenozoic Andean folding.

1. Introduction

Paleozoic paleogeographers generally accept that the southern continents (South America, Africa, India, Antarctica, and Australia) were united as the supercontinent Gondwana between Late Cambrian and Late Triassic times. However, two contrasting interpretations of the Gondwana apparent polar wander (APW) path have yet to be resolved [*Van der Voo*, 1988; *Briden*, 1992]. Because paleomagnetic data from Australia [*Hurley and Van der Voo*, 1987] and Africa [*Hargraves et al.*, 1987] dominate the discussion, we attempted to determine Paleozoic paleomagnetic poles for Gondwana through paleomagnetic study of South America. Samples were taken from Paleozoic red sedimentary strata across the Eastern Cordillera and sub-Andean Belt of Bolivia. Acquisition of a large paleomagnetic data set from this region, however, forced us to the conclusion that the sampled strata have been affected by widespread chemical remagnetization probably during or just preceding Cenozoic folding.

The results of this study are of significance to paleomagnetic analyses undertaken elsewhere. We report here well-determined site-mean characteristic directions of natural remanent magnetism (NRM) from some Paleozoic red sedimentary rocks which have been interpreted previously to possess a primary magnetization [*Ernesto et al.*, 1988]. Through comparison of paleomagnetic data from widely distributed collecting locations, application of a modified conglomerate test, and observation of consistent characteristic directions throughout a Devonian through Permian age section, the remagnetization of these rocks can be documented. Less thorough paleomagnetic study could lead to the erroneous conclusion that a primary Paleozoic NRM has been retained by these strata in the Eastern Cordillera and sub-Andean Belt of Bolivia.

Paper number 98JB02848.
0148-0227/98/98JB-02848$09.00

2. Tectonic and Geologic Setting

Sedimentation in Bolivia was almost exclusively marine from the Late Cambrian through the Permian, and predominantly continental in the Mesozoic and Cenozoic [*Sempere*, 1995]. Extensional deformation of western South America began in the early Mesozoic. Relatively little compressional tectonic activity occurred before Andean-related shortening began along the Pacific margin ~89 Ma. Beginning in the Late Cretaceous, a varying compressional regime along this margin resulted in the development of a number of foreland basins, as is evidenced by typical foreland successions in the Andes. Overall, the development of an external foreland basin controlled by nearby easterly propagating deformation, beginning as early as the Paleogene, is a major feature of the Cenozoic evolution of the Andes [*Sempere et al.*, 1997]. This deformation continues today, with an active foreland basin existing east of the Andes.

The formation of the Bolivian orocline has been an active focus of research for the past decade and modifies the record of simple compressional deformation in South America [e.g. *Roperch and Carlier*, 1992; *Butler et al.*, 1995; *Randall et al.*, 1996]. Crustal scale block rotations, counterclockwise to the north and clockwise to the south, have been documented in Bolivia, Chile, and Peru [*Randall et al.*, 1996]. Rotations documented through paleomagnetic study of Upper Cretaceous to Tertiary strata have been observed in the region (Figure 1). Documented rotations within the study area range in magnitude from 5° to 65° [*Butler et al.*, 1995].

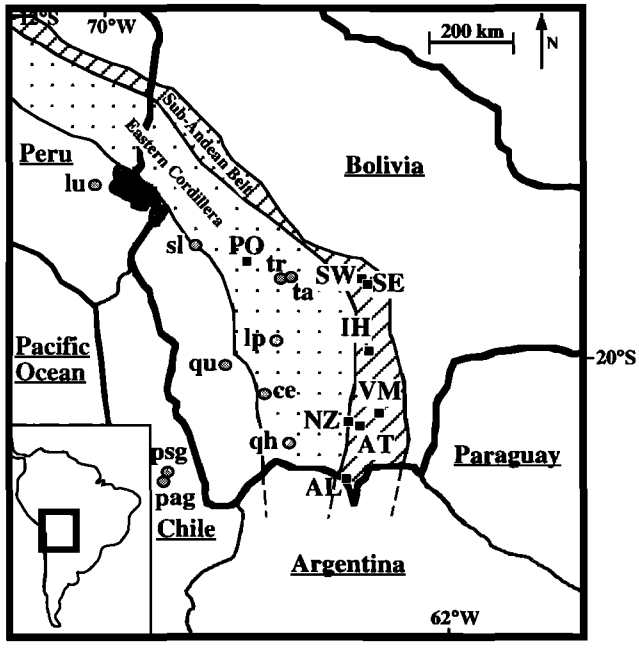

Figure 1. Map showing site localities and locations for which vertical axis rotations have been documented in and near the study area. Stippled area, Eastern Cordillera; lined area, sub-Andean Belt. Black squares are site localities for this study. PO, Pongo; IH, Inca Huasí; SW, Samaipata West; SE, Samaipata East; AL, Alarache; NZ, Narvaez; AT, Abra Tapecua; VM, Villamontes. Refer to Table 1 for a list of the formations sampled at each of these localities. Gray circles are localities from which paleomagnetic data are available to constrain vertical axis rotations [*Randall et al.*, 1996; *Hartley et al.*, 1992; *Butler et al.*, 1995]. Abbreviations are qh, Quebrada Honda; sl, Salla; pag, Paciencia Group; psg, Purilactis Group; ta, Tiupampa; lu, Laguna Umayo; lp, La Palca; qu, Quehua; ce, Cerdas.

Eight stratigraphic units ranging in age from Early Devonian to Early Triassic were sampled for this project. Precise site localities and unit ages are listed in Table 1. Although the sampled strata were primarily red beds, the depositional histories of these units are distinct, with depositional environments ranging from fluvial to glacio-marine. Site locations were selected on the basis of grain size (fine-grained units are preferable for paleomagnetic analysis) and red to purple pigmentation. A general description of the depositional and lithologic nature of sampled units is provided here. Descriptions of "local" lithologies refer to the nature of the formation at the sampling locality. Figure 2 illustrates formation names, ages, and lithologic correlations for the Eastern Cordillera and sub-Andean Belt.

2.1. Vilavila Formation

The Lower Devonian (Lochkovian) Vilavila and Santa Rosa formations were deposited in fluvial to shallow marine environments. The Vilavila Formation has been mapped over a much smaller area than the Santa Rosa, namely, west and northeast of Oruro, and consists of mainly red, cross-bedded to massive, coarse to fine sandstones intercalated with red siltstones and mudstones. The Santa Rosa Formation consists of similar sedimentary facies but does not show red pigmentation. Slumped beds occurring in both the Vilavila and Santa Rosa, in the study area and elsewhere, are indicative of syndepositional tectonic activity [*Sempere*, 1995].

2.2. Mississippian Units

We sampled the Mississippian Itacua, Tupambi, Taiguati, Escarpment and San Telmo formations within the central and southern sub-Andean Belt of Bolivia. These stratigraphic units were deposited in a glacio-marine environment while the region was in a period of tectonic instability [*Sempere*, 1995]. The uppermost Famennian to lower Mississippian Itacua Formation consists of predominantly coarse, moderately-well lithified red sandstones with a few interbeds of poorly lithified fine sandstone to mudstone. Regardless of grain size, sandstones from the Itacua commonly have a red muddy matrix. The Itacua is approximately 50 m thick in the section sampled at Villamontes.

The lower Mississippian Tupambi Formation consists of coarse to fine sandstones, commonly conglomeratic, deposited in cross-bedded to massive channels and alternating with subordinate and thinner red fine sandstone to siltstone beds. The sandstones are porous and permeable and are known to form hydrocarbon reservoirs in the sub-Andean Belt [*Sempere*, 1995]. At Villamontes, the Tupambi Formation is about 350 m thick. The surfaces of many sandstone beds in the Tupambi Formation contain abundant visible hematitic zones. These

Table 1. Sample Localities and Formation Names

Location	Latitude, °S	Longitude, °W	Unit Name	Unit Age	Site Names
Villamontes	21.27	63.54	Itacua Fm	D	IT001-003
Villamontes	21.27	63.54	Tupambi Fm	M	TP001-017
Villamontes	21.27	63.54	San Telmo Fm	upper M	ST010-022
Villamontes	21.27	63.54	Taiguati Fm	M	TG023-025
Villamontes	21.27	63.54	Vitiacua Fm	P–Tr	VT010-022
Abra Tapecua	21.43	63.93	Ipaguazu Fm	Tr	IZ001-002
Narvaez	21.44	64.26	San Telmo Fm	upper M	ST001-006
Alarache	22.24	64.60	Taiguati Fm	M	TG001-003
Alarache	22.24	64.60	Vitiacua Fm	P–Tr	VT001-004
Samaipata-East	18.78	63.82	Escarpment Fm	M	EC001-003
Samaipata-West	18.15	63.93	Taiguati Fm	M	TG004-009
Inca Huasi	19.83	63.73	Taiguati Fm	M	TG020-022
Pongo	17.71	66.58	Vilavila Fm	D	VV001-015

Unit Age lists regional ages of sampled units where D, Devonian; P, Permian; Tr, Triassic; and M, Mississipian. Fm, Formation.

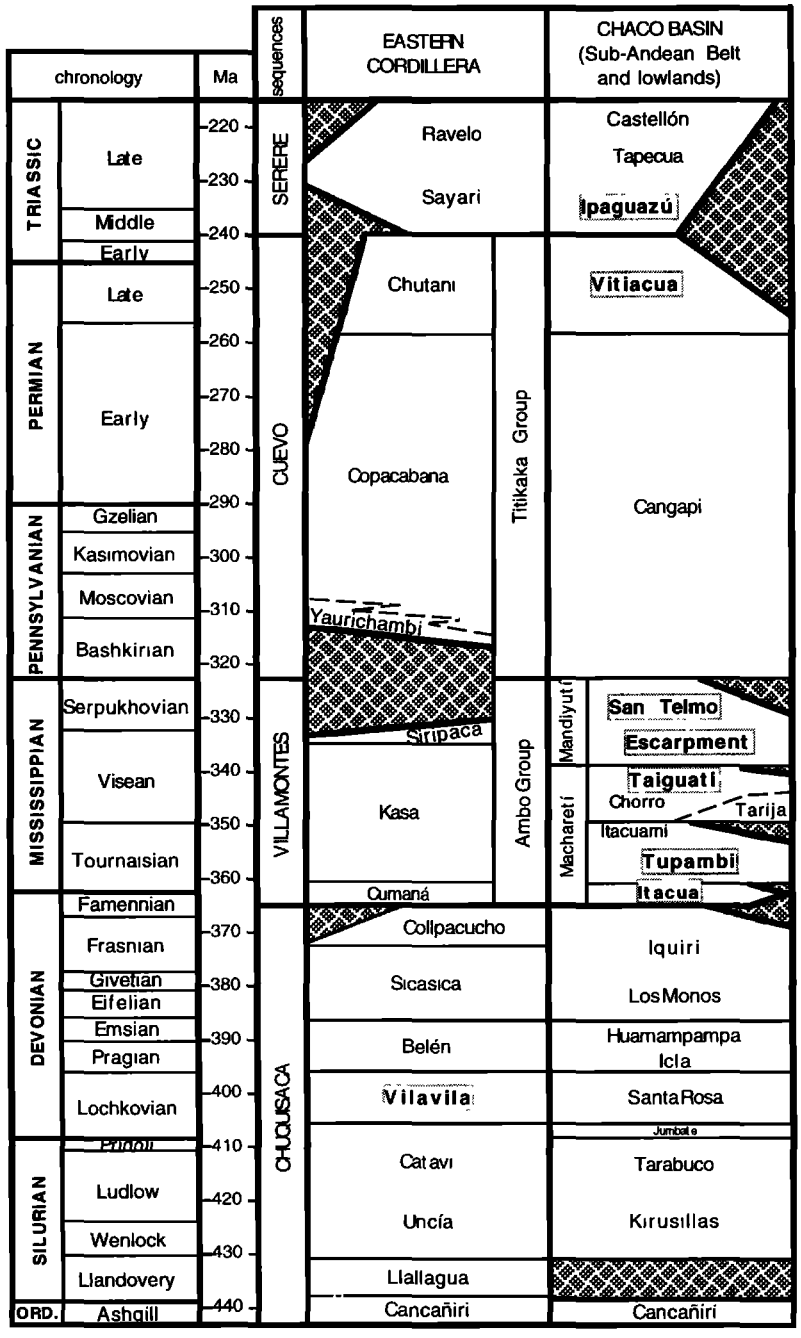

Figure 2. Stratigraphic names and correlation for the sub-Andean and Andean zones of Bolivia.

zones are probably due to alteration of this unit caused by fluids circulating through the sandstones.

The middle Mississippian Taiguati Formation consists of generally reddish sandy to muddy sediment derived predominately from underlying formations. At Villamontes, this unit is approximately 100 m thick and appears mostly as a series of well-cemented bluish-gray mudstones.

The Escarpment and San Telmo formations are now considered to be Late Mississippian [*Sempere*, 1995]. The Escarpment Formation consists of thickly bedded, commonly conglomeratic, massive to cross-bedded sandstones that were deposited as debris flows, grain flows, turbidites, and slumps. The San Telmo Formation consists of generally thinner and finer sandstones alternating with red siltstones to mudstones. Water escape structures are commonly observed in the sandstones of the lower and middle parts of the unit, which also frequently display turbidite facies. Sandstones in the upper part of the unit were deposited in shallower environments with fluvial facies present at Villamontes. Because of the good porosity and permeability of these sandstones, both the Escarpment and San Telmo formations serve as important hydrocarbon reservoirs in the sub-Andean Belt. At Villamontes, some beds of the San Telmo Formation contain hematitic spots similar to those observed in the Tupambi Formation.

2.3. Vitiacua Formation

The Upper Permian–Lower Triassic Vitiacua Formation was deposited in a mainly restricted-marine basin. The limy mud-

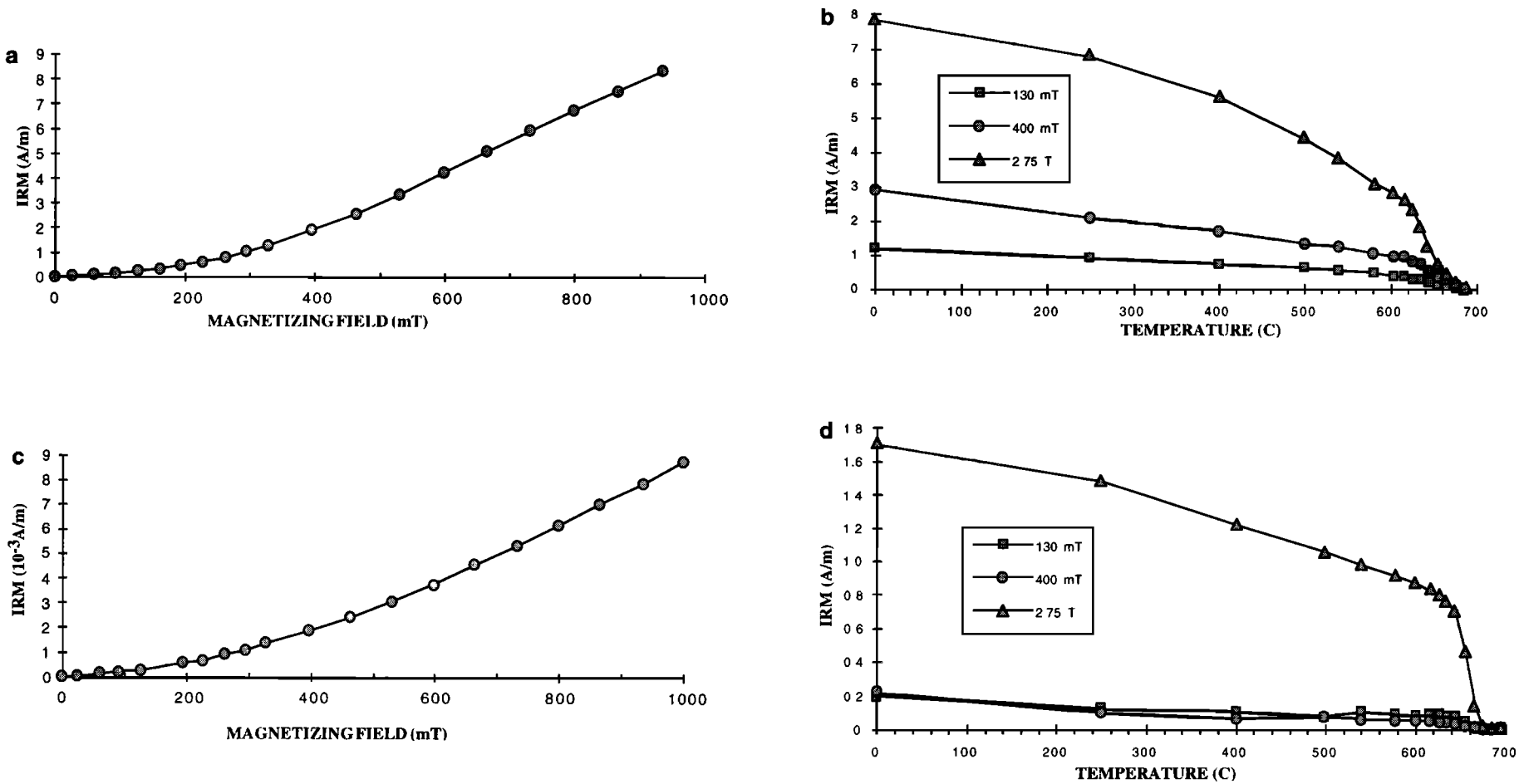

Figure 3. Coercivity spectrum analyses for representative samples from the Alarache locality. (a, c) Acquisition of isothermal remanent magnetism (IRM) as a function of magnetizing field. (b, d) Thermal demagnetization of three coercivity fractions as a function of temperature. Figures 3a and 3b are from the Taiguati Formation. Figures 3c and 3d are from the Vitiacua Formation.

stones of the lower Vitiacua Formation mark a major transgression which affected much of Gondwana [*Sempere et al.*, 1992]. The upper Vitiacua Formation consists predominantly of cherty dolomitic carbonate. At Villamontes this unit is a very thinly bedded to laminated succession of dominantly pink siliceous carbonate, including gray, blue, and white cherts and interbedded with red fine-grained siliceous layers. Sampling was concentrated within the pink to red layers or encompassed entire red laminations within the lighter cherty beds. Red siliceous concretions present within the upper part of the section were also sampled.

2.4. Ipaguazú Formation

The Triassic Ipaguazú Formation is recognized mainly in the southern sub-Andean Belt, where it can be observed up to 400 m thick in places. It consists of red-brown mudstones, siltstones, and fine to medium-grained sandstones, with thick evaporites locally. These facies were deposited in alluvial to playa-lake environments. The sampled strata occur in a relatively thick succession of alternating thickly bedded muddy sandstones and finely bedded to laminated mudstones.

3. Paleomagnetism

3.1. Procedures and Rock Magnetic Analyses

Paleomagnetic samples were obtained from Devonian and Late Paleozoic strata at eight localities within the Eastern Cordillera and sub-Andean regions of Bolivia (Figure 1 and Table 1). Using standard paleomagnetic coring methods, oriented samples were collected from a total of 98 sedimentary beds (= paleomagnetic site with generally eight samples per site) within eight geologic units. Samples were oriented using both magnetic compass and solar compass. No significant deviations were noted between these orientation methods. An additional 14 samples were taken from slumped blocks at one particular level of the Vilavila Formation. The preservation of recognizable bedding in these slump blocks allowed us to use these samples in a modified conglomerate test.

Following sample preparation, all specimens were stored and analyzed in a magnetically shielded room with background field intensity ≤ 200 nT. NRM was measured with a three-axis cryogenic magnetometer (2G model 755R). Thermal demagnetizations at 14 to 18 steps up to 680°C were accomplished using furnaces with magnetic field intensity less than 10 nT in the sample region. Results of thermal demagnetization were analyzed by principal component analysis [*Kirschvink*, 1980], and site-mean directions were determined using the statistical methods of *Fisher* [1953].

Analyses of coercivity spectra of 11 representative samples were performed using the methods of *Dunlop* [1972] and *Lowrie* [1990]. Representative results of isothermal remanent magnetism (IRM) analyses are illustrated in Figure 3. The majority of the samples showed IRM acquisition and thermal demagnetization behaviors similar to those illustrated in Figure 3. For all coercivity fractions, IRM unblocking temperatures are concentrated between 600°C and 680°C, indicating that hematite is the dominant or exclusive ferromagnetic mineral. Ten thin section analyses confirm the presence of hematite in all of the sampled units.

3.2. Paleomagnetic Results

Results of progressive thermal demagnetization of NRM were observed to be highly variable between formations and between localities. The Tupambi and San Telmo formations at Villamontes typically exhibited univectorial behavior with unusually linear decay of vector end points to the origin of vector component diagrams (Figure 4a). Maximum angular deviation (MAD) of line fits to these demagnetization data showed very small values often less than 1° [*Kirschvink*, 1980]. More typically, MAD values for line fits to the thermal demagnetization data were ≤ 5° (Figure 4b). Rarely, thermal demagnetization yielded erratic behavior from which a characteristic magnetization (ChRM) could only be extracted by fitting lines to results from the highest three or four temperature steps (Figure 4c). These line fits resulted in larger MAD values, ranging from 10° to 15°. Specimens exhibiting MAD greater than 15° were removed from further analysis. Finally, specimens from the Vitiacua Formation at Villamontes invariably produced very erratic behavior upon thermal demagnetization. No ChRM directions could be confidently identified from this formation and, accordingly, sites from the Vitiacua Formation collected at Villamontes were dropped from further consideration.

Two criteria were used to reject sites with poorly determined site-mean ChRM directions. Sites with fewer than four single polarity specimens yielding ChRM directions with MAD ≤ 15° were rejected; sites with site-mean 95% confidence limit, α_{95}, greater than 15° were rejected. Seventy-four site-mean ChRM directions pass these criteria and are listed in Table 2. For all but seven of the accepted sites, six or more sample ChRM directions were available for calculating the site-mean direction. Examples of within-site clustering of ChRM directions and ChRM site-mean directions are shown in Figure 5. Some sites yielded unusually well grouped ChRM directions with correspondingly small confidence limits (Figure 5a). Typical sites had site-mean ChRM directions with α_{95} between 5° and 10° (Figure 5b). Amongst the sites passing the selection criteria, the largest site-mean α_{95} was 12° (Figure 5c).

Of the 74 accepted site-mean ChRM directions, only 11 contain normal polarity directions; seven of these sites are from Pongo, two are from Samaipata West, and two are from Villamontes. Site TG008 from Samaipata West contains dual-polarity magnetization with normal and reversed polarity ChRM directions preserved in each of four samples (Table 2). Mean directions of ChRM from the polarity subsets of samples from these two sites are sufficiently well determined to warrant treating each polarity subset as a site-mean ChRM direction in subsequent analyses.

3.3. Field Tests

Systematic examinations of field tests for paleomagnetic stability were fundamental to documenting the secondary nature of the characteristic magnetizations. Particularly critical was application of the conglomerate and fold tests [*Graham*, 1949] using the statistical methods of *Watson* [1956], *Watson and Irving* [1957], and *McFadden* [1990]. Plunge corrections were not required for localities where field tests were applied because folds in the study area extend tens to hundreds of kilometers along strike. Results of the modified conglomerate test applied to the sedimentary layer containing laminated slump blocks within the Early Devonian Vilavila

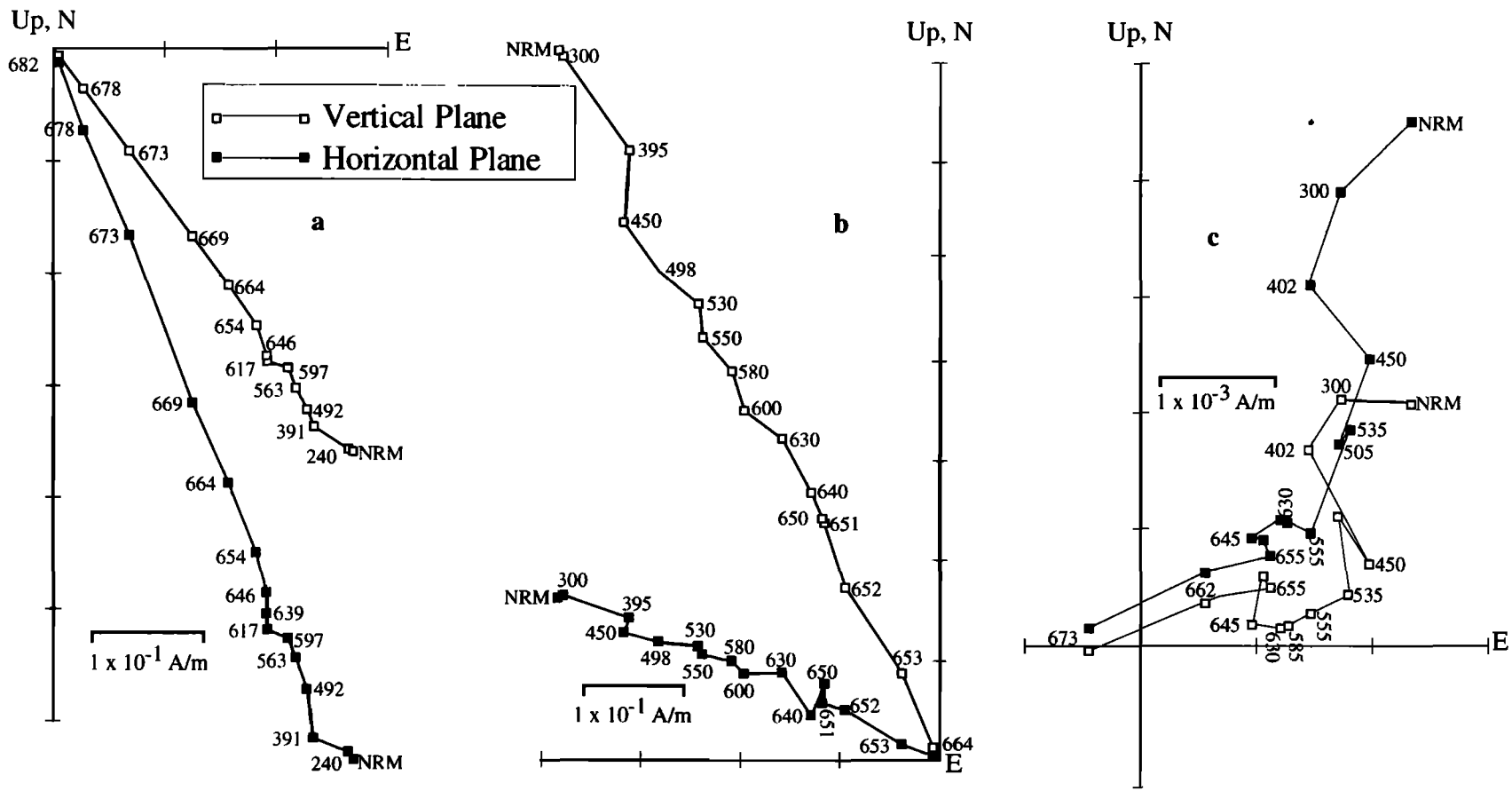

Figure 4. Typical progressive thermal demagnetization results in stratigraphic coordinates. (a) Good result. ST020B from the San Telmo Formation, Villamontes locality. (b) Average result. VV052A from the Vilavila Formation, Pongo locality. (c) Marginal result. VV001F from the Vilavila Formation, Pongo locality. Open squares, vertical-plane projection; closed squares, horizontal-plane projection.

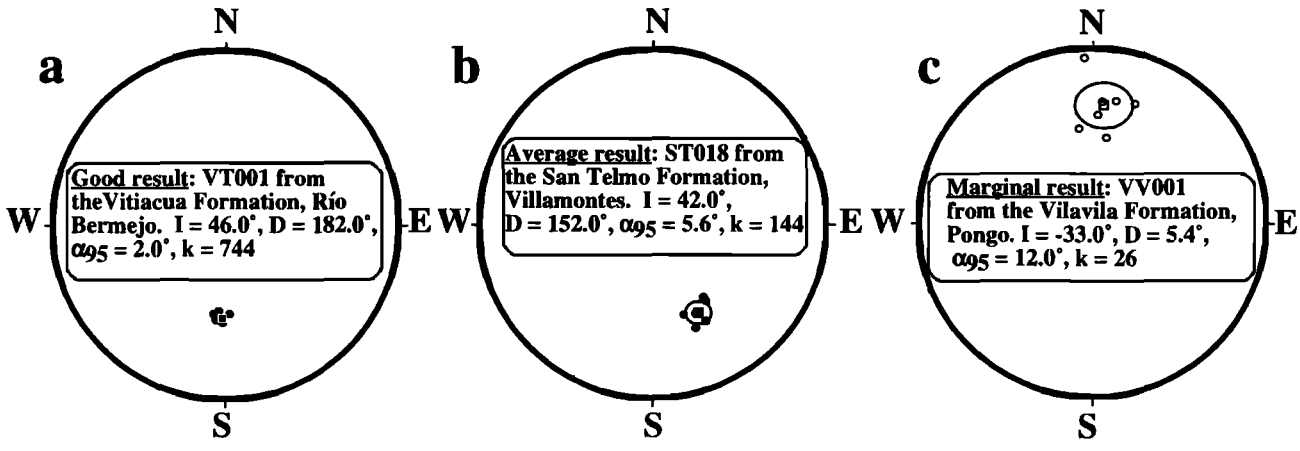

Figure 5. Equal-area projections of sample ChRM directions and site mean ChRM direction, and α_{95} in stratigraphic coordinates for three sites. (a) Good result. VT001 from the Vitiacua Formation, Alarache locality. (b) Average result. ST018 from the San Telmo Formation, Villamontes locality. (c) Marginal result. VV001 from the Vilavila Formation, Pongo locality. Circles, sample ChRM directions; squares, site-mean ChRM directions. Solid symbols are in the lower hemisphere, while open symbols are in the upper hemisphere.

Formation are shown in Figure 6. Fourteen samples from slumped blocks containing recognizable internal bedding yielded ChRM directions. These ChRM directions are tightly grouped in geographic coordinates but disperse upon restoring bedding within each slump block to horizontal. This dispersion of ChRM directions is statistically significant at the 99.9% confidence level and constitutes a negative conglomerate test [*Watson*, 1956]. Because we are unable to determine the extent of vertical axis rotations of these slump blocks, an inclination-only test of dispersion is quantitatively more meaningful than this modified conglomerate test. Accordingly, an inclination-only test, as developed by *McFadden and Reid* [1982], was applied. Application of bedding tilt corrections to the 14 slump block ChRM directions results in a decline in inclination grouping, with a decrease in the estimate of Fisher's precision parameter k from 36.0 in situ to 4.4 after tilt correction. Clearly, the ChRM was acquired after slumping of a laminated and fairly lithified sediment and is therefore a secondary magnetization. Additionally, the in situ directions observed in the slumped blocks are very similar to the normal polarity Vilavila Formation average (Figure 7). Finally, the ChRM directions in geographic coordinates are in directions expected for a Cenozoic magnetization and are unlike those expected for a Devonian magnetization.

Local folding of the Vilavila Formation at the Pongo locality allowed application of the fold test to results from this location. Results of progressive unfolding applied to site-mean ChRM directions are illustrated in Figure 7. A minimum fold test statistic (SCOS) and a maximum k were observed for 80% unfolding, with unfolding values from ~65% to just less than 90% yielding statistically indistinguishable SCOS values [*McFadden*, 1990]. The SCOS value for 100% unfolding falls well above the 95% confidence limit, indicating that the ChRM directions were not acquired when the strata were horizontal or even uniformly tilted. Instead, the ChRM appears to be a synfolding magnetization as observed for many Paleozoic formations of eastern North America [*Scotese et al.*, 1983; *McCabe and Elmore*, 1989]. Apparently the Vilavila Formation acquired its characteristic magnetization at ~80% unfolding when ~20% of the currently observed folding had occurred. These fold test results confirm the secondary nature of the ChRM and further suggest that the Vilavila Formation acquired its characteristic magnetization early in the development of folding. Because this folding regionally affects Paleogene strata, this magnetization is certainly of Cenozoic age.

Analysis of progressive unfolding applied to site-mean ChRM directions from the Villamontes and Narvaez localities are illustrated in Figure 8. Because of the proximity of these localities, a remagnetization of these strata would likely have been roughly coeval. Minimum SCOS was observed at 80% unfolding, with unfolding values from ~65% and ~95%, yielding statistically indistinguishable SCOS values [*McFadden*, 1990]. However, the SCOS value for 100% unfolding falls above the 95% confidence limit. These results clearly indicate a secondary origin for the ChRM and suggest that the Mississippian strata in the Villamontes and Narvaez area also acquired their characteristic magnetization during early stages of folding.

The ChRM directions at 80% unfolding from the Early Devonian Vilavila Formation in the Eastern Cordillera at Pongo and the Mississippian strata at Villamontes and Narvaez are in close agreement (Figures 7 and 8). This observation suggests that the synfolding remagnetization is roughly similar in age across the Eastern Cordillera and southern sub-Andean Belt of Bolivia (Figure 1). As can be seen in Figure 1, the Villamontes and Pongo localities are the southeastern- and northwestern-most sampling localities, respectively. Although field tests cannot be applied to ChRM directions for the intervening localities, the relationship between deformation and remanence acquisition evidenced at the southeastern- and northwestern-most localities suggests that all or most of the magnetizations were acquired during the initial stages of deformation. Accordingly, all directions have been unfolded to 80% (Table 2). Because the magnetization is believed to be acquired contemporaneously across formations in any given locality, location means were calculated by averaging the directions from all of the sites within that locality. The local-

Table 2. Site-Mean Directions for Characteristic Magnetizations

							Geographic Coordinates				80% unfolding			
Site	Strike	Dip	N	J, 10^{-3}A/m	α_{95}, deg	k	I, deg	D, deg	VGP Lat, °N	VGP Long, °E	I, deg	D, deg	VGP Lat, °N	VGP Long, °E
IZ001	013	24	8	4.20	9.8	32.8	-6.5	163.4	-58.0	83.6	-8.3	243.2	-22.3	190.2
IZ002	013	24	7	8.70	14.6	18.0	12.7	149.9	-56.0	53.1	25.3	155.0	-63.9	46.8
EC001	311	10	8	3.30	96.3	1.3	68.8	185.9	-55.7	289.7	61.9	194.8	-62.7	272.2
EC002	306	12	7	8.10	40.0	3.2	46.6	157.2	-66.9	357.1	41.1	164.8	-75.1	4.9
EC003	227	12	6	3.80	99.0	1.4	43.1	187.5	-80.2	252.4	36.6	181.6	-87.8	252.9
VV001	159	41	7	0.64	12.0	26.1	-32 6	5.4	84.9	24.9	-28.7	9.6	80.5	10.2
VV002	159	41	8	2.30	3.4	272.6	39.3	197.7	-72.8	221.7	34.0	202.3	-68.8	209.4
VV003	159	41	6	4.60	7.7	76.6	37.1	193.6	-76.8	218.9	32.2	198.2	-72.7	205.4
VV004	159	41	8	1.30	3.1	312.7	44.6	192.4	-75.7	242.1	39.7	198.4	-72.1	222.1
VV005	159	41	7	1.30	4.0	231.9	44.6	192.6	-75.5	241.9	39.8	198.6	-71.9	222.2
VV006	159	41	7	8.90	3.9	236.3	45.8	196.2	-72.3	238.7	40.4	202.1	-68.6	221.6
VV007	159	41	8	1.10	5.5	100.8	-34.0	2.5	87.4	45.7	-30.5	7.2	83.0	13.8
VV008	159	41	8	4.00	2.3	562.0	-38.9	0.1	85.8	111.7	-37.9	4.0	84.8	67.4
VV009	337	12	7	6.40	3.0	402.2	-36.8	13.6	76.8	37.9	-38.2	12.1	78.0	43.7
VV010	332	18	8	4.50	3.1	317.9	-32.1	23.6	67.6	26.3	-34.9	22.1	69.0	31.0
VV011	348	12	8	5.90	3.3	287.4	-36.9	17.1	73.5	36.2	-38.0	15.6	74.9	39.8
VV012	337	12	8	4.60	2.2	639.4	-34.5	17.6	73.2	30.5	-36.4	14.9	75.7	35.9
VV013	086	03	6	2.70	5.6	143.4	42.2	199.6	-70.5	226.9	41.7	199.4	-70.8	225.9
VV014	086	03	7	2.30	9.2	44.1	50.6	189.2	-74.1	263.7	49.9	189.0	-74.6	262.9
TG004	010	70	5	2.70	7.3	110.3	-29.9	326.2	57.7	204.6	50.9	197.1	-69.5	250.4
TG005	010	70	4	3.00	2.8	1056.6	8.0	137.7	-46.3	39.7	46.7	161.9	-70.7	352.3
TG006	010	70	7	2.70	4.6	173.4	8.3	134.2	-43.1	37.7	49.4	158.7	-67.7	261.0
TG007	010	70	4	2.90	8.2	126.8	2.1	126.1	-34.4	37.7	49.9	143.0	-54.2	358.4
TG008A	358	75	4	12.0	3.3	779.0	10.3	136.6	-45.7	37.6	40.8	165.0	-75.0	3.2
TG008B	358	75	4	3.40	6.7	187.7	6.5	293.9	21.5	217.2	-45.8	306.5	40.2	185.4
TG009	358	75	5	2.20	6.2	155.3	11.2	298.9	25.2	221.7	-39.2	308.4	41.6	192.2
TG001	209	82	8	18.0	7.5	55.7	13.9	270.6	-2.1	212.1	61.3	225.2	-47.5	244.6
TG002	209	82	8	16.0	5.0	124.2	18.4	258.8	-13.8	210.1	52.2	210.1	-61.4	233.6
TG003	209	82	7	6.00	3.8	248.5	26 8	248.0	-25.4	211.0	44.3	194.6	-76.2	224.1
VT001	198	83	8	7.10	2.0	745.3	15.9	243.6	-27.5	203.1	47.7	200.0	-70.8	229.5
VT002	195	83	7	1.60	4.1	218.0	21.3	239.6	-32.1	204.7	48.2	188.9	-79.4	248.3
VT003	198	83	8	6.20	2.3	592.3	13.2	239.6	-30.7	199.9	43.1	201.9	-69.8	217.8
VT004	196	81	8	1.40	4.1	187.6	13.1	243.5	-27.0	201.5	48.3	204.7	-66.7	228.2
ST001	030	18	8	7.50	4.0	188.2	34.8	172.2	-82.3	41.5	42.7	182.0	-86.2	267.2
ST002	007	17	8	19.0	6.3	79.3	38.1	156.6	-68.2	21.5	43.9	167.4	-77.7	3.1
ST003	027	28	7	4.00	4.3	196.6	44.1	165.0	-75.6	5.1	55.7	188.5	-73.4	271.0
ST004	027	28	8	5.70	8.2	46.3	28.4	171.2	-79.5	61.3	39.5	184.6	-85.6	219.3
ST005	027	28	8	7.80	5.1	117.5	27.1	155.4	-65.6	38.5	42.3	165.4	-76.2	10.3
ST006	029	20	6	5.80	8.6	61.3	46.7	130.8	-45.1	6.4	62.2	136.5	-47.9	343.8
TG020	001	88	8	3.90	23.8	6.4	-7.7	114.7	-21.6	39.0	-54.1	313.8	46.8	176.4
TG021	001	88	7	7.30	2.3	661.9	-8.8	125.0	-30.8	44.4	-46.1	323.8	56.1	186.3
TG022	001	88	7	3.90	3.6	285.3	-7.3	118.8	-25.5	40.6	-51.6	319.2	51.6	179.0
IT001	202	31	6	1.40	12.5	29.9	56.5	203.8	-64.0	249.1	48.0	147.0	-59.2	5.1
ST010	220	46	6	32.0	11.6	34.5	60.6	240.2	-35.9	243.2	53.0	180.0	-77.7	296.5
ST011	214	46	6	42.0	5.0	177.8	42.6	214.3	-58.4	219.4	33.0	185.3	-84.0	174.1
ST012	214	46	6	33.0	6.0	124.4	48 6	206.9	-64.4	230.9	33.5	175.9	-85.1	63.2
ST013	214	46	5	160	6.8	127.1	49.6	197.2	-72.1	240.7	29.8	169.7	-78.9	53.2
ST014	201	42	6	170	4.3	240.9	60.9	227.2	-45.5	245.4	57.8	166.1	-69.1	328.2
ST015	212	44	6	130	7.0	91.9	57.9	216.3	-54.4	243.8	45.7	171.3	-80.1	348.3
ST016	205	42	6	76.0	5.9	129.5	48.6	211.2	-60.8	229.4	41.6	176.6	-85.9	345.5
ST017	205	42	6	51.0	4.9	188.9	44.8	213.4	-59.1	222.7	40.1	181.6	-87.8	253.3
ST018	205	42	6	80.0	5.6	144.4	63.3	206.4	-58.0	259.9	48.6	157.8	-68.3	359.4
ST019	205	42	6	49.0	6.6	105.1	48.0	226.2	-47.7	226.8	48.8	186.4	-79.8	263.5
ST020	211	44	6	87.0	7.6	78.4	60.0	204.4	-61.5	255.6	42.4	163.3	-74.3	11.3
ST021	208	44	5	62.0	9.3	69.3	44.1	220.7	-52.6	221.7	41.3	186.8	-83.3	229.0
ST022	209	46	5	92.0	8.0	92.5	43.5	226.7	-47.1	221.3	43.1	190.2	-79.9	230.5
TP001	208	31	6	9.20	7.4	83.0	49.6	209.1	-62.4	231.8	44.1	182.6	-84.8	269.5
TP002	208	31	6	7.60	5.5	151.4	38.8	196.0	-75.1	211.7	30.1	179.7	-84.9	113.2
TP003	208	31	6	29.0	4.7	203.6	35.0	198.3	-72.8	203.2	27.6	183.6	-82.5	144.4
TP004	208	31	6	25.0	4.6	210.8	43.2	205.4	-66.4	220.8	37.4	184.5	-85.8	202.5
TP005	208	31	6	15.0	1.9	1283.5	46.1	202.5	-68.6	227.7	38.8	180.3	-89.3	272.7
TP006	208	31	6	7.50	5.1	174.9	46.6	204.3	-67.0	228.0	39.9	181.3	-88.4	256.3
TP007	208	31	6	4.30	1.5	1935.4	47.4	213.4	-58.9	226.8	44.0	187.6	-81.7	240.8
TP008	208	31	6	7.60	4.6	208.9	47.8	205.7	-65.6	229.8	41.4	181.5	-87.1	267.9
TP009	208	31	6	2.50	7.5	80.4	46 0	206.8	-64.9	225.9	40.3	183.6	-86.2	234.3
TP010	208	31	6	26.0	2.1	1043.7	49.6	204.5	-66.2	234.1	42.4	179.2	-86.6	309.0

Table 2. (continued)

Site	Strike	Dip	N	J, 10^{-3}A/m	α_{95}, deg	k	Geographic Coordinates I, deg	Geographic Coordinates D, deg	Geographic Coordinates VGP Lat, °N	Geographic Coordinates VGP Long, °E	80% unfolding I, deg	80% unfolding D, deg	80% unfolding VGP Lat, °N	80% unfolding VGP Long, °E
TP011	202	31	6	13.0	8.1	70.0	57.6	207.8	-60.7	248.0	52.1	172.2	-76.6	326.0
TP012	202	31	6	4.20	7.3	84.4	39.6	202.0	-69.5	213.9	35.4	182.9	-86.8	174.8
TP013	202	31	6	6.80	10.9	39.0	-52.3	41.8	51.3	53.0	-53.6	8.0	75.3	89.4
TP014	202	31	6	1.60	11.0	38.1	-39.3	2.4	87.5	51.1	-27.8	347.5	76.5	233.1
TP015	202	31	6	15.0	10.1	45.3	41.9	187.1	-82.8	231.6	31.7	169.7	-79.4	47.6
TP016	202	31	6	10.0	3.3	402.1	53.6	205.0	-64.5	242.1	48.0	174.4	-80.7	328.4
TG023	210	36	6	71.0	5.5	147.7	69.8	181.6	-57.6	294.7	48.0	147.0	-59.2	5.1
TP017	202	31	6	12.0	10.8	39.8	50.2	218.1	-54.6	230.4	50.5	187.3	-78.1	264.7

Site, site number; strike and dip, measured using the right-hand rule; N, number of samples from the site used for determinations of site-mean directions; J, geometric mean of the intensity of the characteristic component of the magnetization; α_{95}, 95% confidence limit for the mean direction computed from *Fisher* [1953] statistics; k, best estimate of Fisher's precision parameter; I and D, inclination and declination of the site-mean direction; Lat and Long, latitude and longitude of the virtual geomagnetic pole calculated from the site-mean direction. Results are listed in both geographic and 80% unfolding coordinates.

ity mean directions were then used to calculate locality mean paleopoles (Table 3).

3.4. Previous Results

Two paleomagnetic studies have been conducted on some of the same rock units and in similar localities as studied in the current project. *Creer* [1970] measured an NRM from the Taiguati Formation near the town of Samaipata, which is located between our two Samaipata sampling localities. This magnetization was interpreted as primary, although it is nearly concordant with Tertiary field directions. *Ernesto et al.* [1988] studied a series of Carboniferous sections across the sub-Andean Belt, including one section near Villamontes. They concluded that these rocks carry a primary Carboniferous magnetization on the basis of both agreement with the *Creer* [1970] pole and increased clustering upon tectonic correction. We applied the *McFadden* [1990] fold test to the data acquired by *Ernesto et al.* [1988] and found no statistically significant changes in SCOS values at any degree of unfolding. Additionally, their "Carboniferous" pole falls close to the Tertiary APW path for South America, supporting our belief that these data are representative of Tertiary, not Carboniferous directions.

4. Discussion

The paleomagnetic analyses detailed above indicate that all Paleozoic strata sampled in this study have been remagnetized, probably during early stages of Andean deformation. Our sampling localities cover large areas of the exposed mid-Paleozoic strata of Bolivia (Figure 1), and we find no evidence that primary magnetizations have been retained by these rocks. Instead, detailed application of field tests for paleomagnetic stability document the secondary origin of the characteristic magnetization. In other regions, such as the Appalachians of North America, where remagnetizations have been documented [*McCabe and Elmore*, 1989; *Stamatakos et al.*, 1996], analyses of paleomagnetic pole positions determined from remagnetized rocks have been used to determine an age of remagnetization. For several reasons, age assignment for the remagnetization of Paleozoic strata in Bolivia is possible with only limited precision.

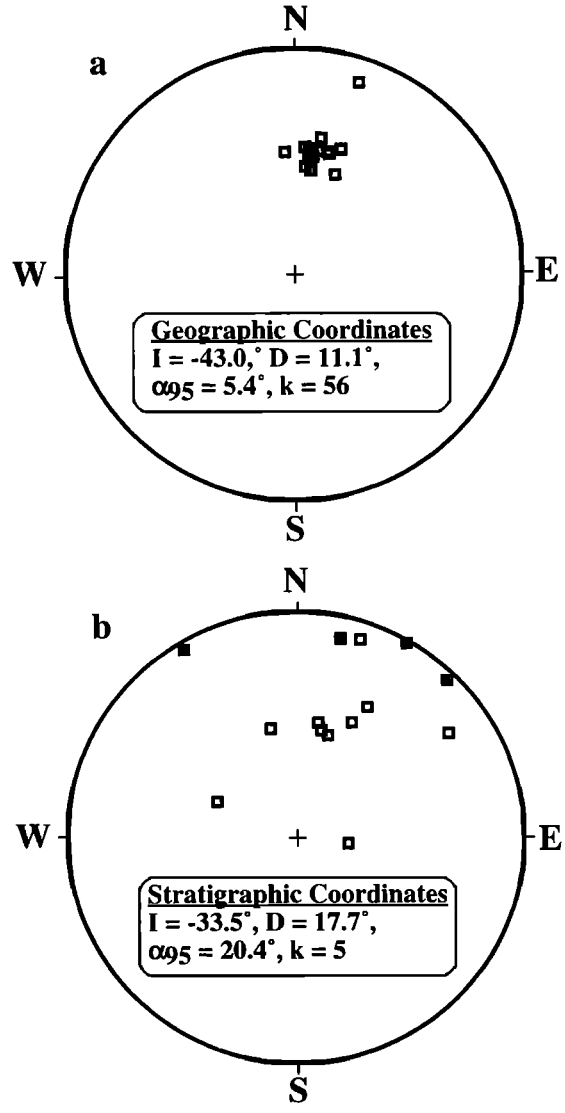

Figure 6. Conglomerate test results from the Vilavila Formation, Pongo locality. Equal-area projections show sample ChRM directions from slump blocks in (a) geographic coordinates and (b) stratigraphic coordinates. Solid squares are lower-hemisphere directions, while open squares are upper-hemisphere directions.

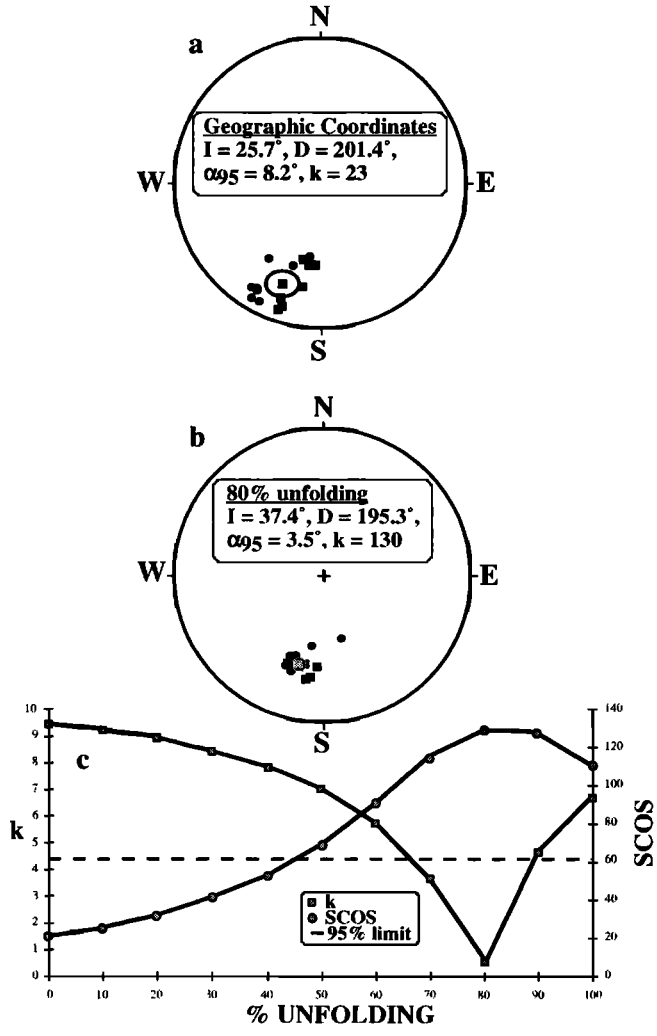

Figure 7. Fold test results from the Vilavila Formation, Pongo locality. Equal-area projections of site-mean ChRM directions are shown in (a) geographic coordinates and (b) at 80% unfolding. (c) SCOS and k are the fold test statistic and the estimate of Fisher's precision parameter, respectively [*McFadden*, 1990]. Solid circles are normal polarity site means reflected through the origin. Solid squares are reverse polarity site means. Squares are location mean directions. Ovals of 95% confidence are plotted about the location means.

Factors limiting the precision with which the characteristic directions can be used to infer age of remagnetization and tectonic disturbance subsequent to remagnetization include the following: (1) The major variation in bedding attitudes within the Pongo sampling area allows the percent of folding at remagnetization to be fairly tightly constrained to 20% folding (Figure 7). However, the major sampled stratigraphic sequence at Villamontes is nearly homoclinal and that section has only a modest contrast of bedding attitude with other sampling localities in that region. Accordingly, assignment of percent folding at the time of remagnetization of Paleozoic strata at Villamontes lacks precision (Figure 8). (2) The magnitude of APW as viewed from South America is modest during Mesozoic and Cenozoic time [*Irving and Irving*, 1982; *Besse and Courtillot*, 1991]. Therefore only very low resolution is possible when inferring ages of magnetization by matching observed paleomagnetic poles with the South American APW path. (3) Cenozoic Andean deformation has involved tectonic vertical axis rotations which affected large regions of the Andes. Paleomagnetic studies have begun to reveal the timing, magnitudes, and spatial extent of these rotations [*Roperch and Carlier*, 1992; *Butler et al.*, 1995; *Randall et al.*, 1996]. However those patterns are not simple, and vertical axis rotations in some areas, most notably the sub-Andean Belt, remain to be determined.

While accepting the restrictions and uncertainties outlined above, we believe basic inferences about age and mode of remagnetization of Paleozoic strata in the Eastern Cordillera and sub-Andean Belt of Bolivia can be drawn from our paleomagnetic results when coupled with geologic observations. From two lines of evidence there seems little doubt that the observed remagnetization is Cenozoic. First, the synfolding

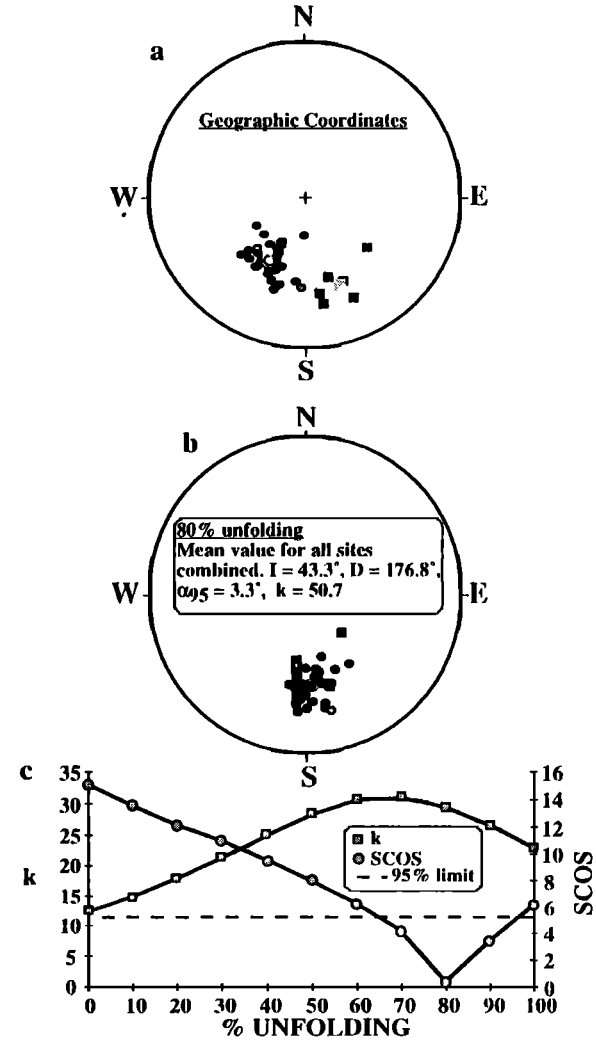

Figure 8. Fold test results for the San Telmo Formation, Villamontes and Narvaez localities in (a) geographic coordinates and (b) at 80% unfolding. (c) SCOS and k are the fold test statistic and the estimate of Fisher's precision parameter, respectively [*McFadden*, 1990]. Site mean directions are shown by circles for Villamontes and squares for Narvaez. Gray-filled symbols are normal polarity site means reflected through the origin. Solid symbols are reverse polarity site means. Gray symbols are formation means for both localities. Ovals of 95% confidence are plotted about the location means.

Table 3. Locality Means in Geographic and 80% Unfolding Coordinates and Calculated Paleopoles

	80% unfolding Coordinates							Geographic Coordinates							
Locality	I, deg	D, deg	α_{95}, deg	k	Lat, °N	Long, °E	A_{95}, deg	I, deg	D, deg	α_{95}, deg	k	Lat, °N	Long, °E	A_{95}, deg	Sites
Villamontes	41.0	177.5	5.0	26.98	-82.8	19.0	3.3	50.1	208.0	3.5	52.35	-62.7	234.5	4.1	32
Samaipata West	48.3	153.3	12.9	22.82	-70.6	324.0	17.0	5.9	130.2	13.1	22.03	-39.2	37.2	10.0	7
Pongo	37.4	195.3	3.5	129.96	-76.9	227.3	3.7	26.2	200.7	9.1	20.10	-70.6	197.6	6.8	14
Narvaez	48.8	172.6	12.2	31.26	-78.2	310.2	15.7	37.3	159.4	11.9	32.90	-0.4	22.3	12.7	6
Alarache	49.7	202.5	6.9	76.46	-82.3	265.4	6.9	17.8	249.1	9.1	44.56	-22.8	206.2	8.8	7
Abra Tapecua	11.7	201.6	–	–	-65.4	62.0	30.4	3.1	156.7	53.3	24.10	-57.9	67.9	37.0	2
Inca Huasí	50.7	139.2	7.9	244.90	-66.3	333.1	5.4	-8.0	119.5	8.0	241.45	-26.0	41.2	8.0	3
Samaipata East	47.1	178.4	25.8	23.90	-80.1	296.1	27.1	53.7	175.5	27.2	21.62	-72.0	306.6	32.3	3

Sites, total number of sites used in the calculations; α_{95} and A_{95}, 95% confidence limit for the mean direction and the mean pole computed from *Fisher* [1953] statistics; k, best estimate of Fisher's precision parameter; I and D, inclination and declination of the site-mean direction; Lat and Long, latitude and longitude of the virtual geomagnetic pole calculated from the site-mean direction. Results are listed in both geographic and 80% unfolding coordinates.

nature of the remagnetization connects the timing of remagnetization with that of fold and thrust belt development in the Andes. Major phases of fold and thrust belt development began during late Oligocene in the Eastern Cordillera and continued into the Pliocene or Quaternary in the sub-Andean Belt [*Sempere et al.*, 1990; *Baby et al.*, 1994]. Second, the paleomagnetic pole positions determined from the characteristic paleomagnetic directions at 20% folding generally agree with the Cenozoic APW path for South America. Figure 9 illustrates the Cenozoic APW path for South America, as well as expected Late Devonian and Late Carboniferous poles. Only two paleomagnetic poles determined from our data set, Villamontes (VM) and Pongo (PG), have small enough confidence limits to rigorously compare with the South American APW path (Figure 9). Both of these poles, as well as the virtual geomagnetic poles (VGP) from other areas, fall well away from expected Paleozoic poles (Table 3 and Figure 9). The paleomagnetic pole from Villamontes falls on the 60–70 Ma portion of the APW path while the pole from Pongo is nearest the 10 Ma portion of the path. The discordance of the Pongo pole suggests a small amount of rotation at this locality, but again we are reluctant to be more quantitative based upon this data set alone.

Along with the above arguments for a Cenozoic age of remagnetization of Paleozoic strata in Bolivia, it is also important to point out what we believe should not be inferred from our observations. A general age assignment of remagnetization to Cenozoic time is reasonably clear. However, attempts to resolve age differences in remagnetization between the sampled areas and perhaps infer details of fluid migration are beyond the resolution of the available data. Uncertainties in the percent unfolding at the time of remagnetization and possible vertical axis rotations simply prevent any meaningful inferences beyond our first-order conclusion that the remagnetization occurred during the Cenozoic. Given the sparse current knowledge of vertical axis rotations in the Andes coupled with structural and age uncertainties for the remagnetization directions reported here, it would be stepping well beyond the available data to use the observed paleomagnetic directions to infer magnitude or even sense of vertical axis rotations subsequent to remagnetization.

Drawing upon paleomagnetic, rock magnetic, structural geologic, and geochemical studies of the remagnetization which affected the Appalachian region of North America during the late Paleozoic time, we conclude with speculations on the process of remagnetization of the Paleozoic strata of Bolivia. In North America, fluids propagating from the fold and thrust belt of the Appalachian Orogeny remagnetized siliciclastic and carbonate rocks across the orogen and onto the craton [*McCabe and Elmore*, 1989]. Orogenic fluid migration, including water and hydrocarbons, in the Appalachians may have

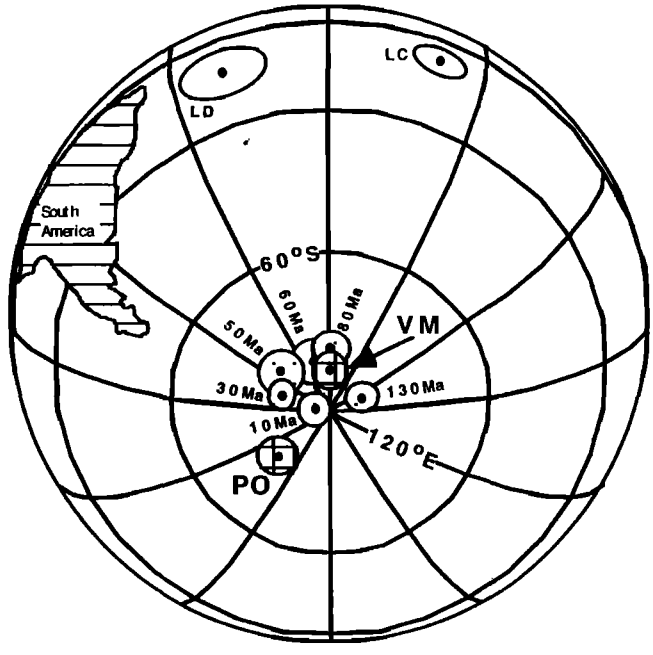

Figure 9. Hatched circles are 95% confidence limits (A_{95}) for locality mean paleopoles from Villamontes (VM) and Pongo (PG) localities. Open circles are the A_{95} for the Late Carboniferous (LC [*Irving and Irving*, 1982]; -9.2°N, 21.0°E, A_{95} = 5.0°) and Late Devonian (LD [*Hurley and Van der Voo*, 1987]; -13.9°N, 339.8E, A_{95} = 8.0°) poles. Stippled circles are the A_{95} for the poles which make up the Late Cretaceous–Tertiary Apparent Polar Wander (APW) path [*Butler et al.*, 1995; *Roperch and Carlier*, 1992; *Raposo and Ernesto*, 1995]: 10 Ma, -86.9°N, 273.5°E, A_{95} = 3.0°; 30 Ma, -80.5°N, 287.3°E, A_{95} = 2.7°; 50 Ma, -78.9°N, 307.0°E, A_{95} = 4.3°; 60 Ma, -80.5°N, 340.7°E, A_{95} = 4.2°; 80 Ma, -78.9°N, 3.0°E, A_{95} = 3.1°; 130 Ma, -83.8°N, 60.3°E, A_{95} = 4.3°. Mid-Paleozoic paleopoles have been rotated from African into South American coordinates by counterclockwise rotation of 57° about an Euler pole at 44°N, 329.4°E [*Irving and Irving*, 1982].

been driven by either a "squeegee" effect of the developing thrust belt [*Oliver*, 1986] or in response to a gravitationally driven hydraulic gradient [*Garven and Freeze*, 1984; *Lawrence and Cornford*, 1995]. The synfolding remagnetization of Paleozoic strata over large areas of Bolivia during Andean deformation could have followed a similar sequence of processes. All Paleozoic strata sampled in this study were at some time buried below the active Andean foreland basin as evidenced by geologic relationships and hydrocarbon accumulations present in some units. Progressive west to east propagation of the fold and thrust front from a late Oligocene position in the Eastern Cordillera to its present location within and east of the sub-Andean Belt drove fluid migration with attendant chemical remagnetization. The suggestion from the paleomagnetic data that remagnetization occurred when the beds were only 20% deformed is explained by a ChRM which remained stable during subsequent fold and thrust deformation. This stability is likely if orogenic fluid composition did not change dramatically during subsequent deformation [*Lawrence and Cornford*, 1995].

5. Conclusions

The paleomagnetic data presented here indicate that Paleozoic units across the Eastern Cordilleran and sub-Andean Belt of Bolivia have been remagnetized during Cenozoic deformation. The lack of preservation of original magnetizations and the pervasive remagnetization documented here suggest that primary Paleozoic magnetizations are probably not preserved in sedimentary strata in this region. Future attempts to obtain primary paleomagnetic directions from Paleozoic rocks of the Andes should focus on less deformed regions, perhaps in the forebulge region of the active foreland basin. Finally, the documentation of this remagnetization reaffirms the critical importance of multiple field tests of paleomagnetic stability when applying paleomagnetic methods to rocks in orogenic zones.

Acknowledgments. We thank Brigette Martini, Scott Balay, and Rob Feyerharm for major technical assistance with laboratory measurements and Tom Moore for assistance with computer programs. Larry Marshall provided valuable field assistance during early stages of this project. Critical logistical assistance in Bolivia was provided by Ramiro Suárez. Genaro Montemurro, Jaime Oller, and Miguel Cirbián also assisted during our time in Bolivia. The practiced eye of Rob Van der Voo first spotted the possibility of synfolding magnetizations in our data. We thank Rob for urging us to carefully evaluate the case for synfolding magnetization which turned out to be such fertile territory. Norm Meader provided major assistance in preparation of the camera ready copy. This research was supported by National Science Foundation grant EAR 9316414 and National Geographic Society grant 5743-96.

References

Baby, P., B. Guillier, J. Oller, E. Mendez, G. Montemurro, and D. Zubieta, Sintesis estructural del Subandino boliviano, in *XI Congreso Geologico Boliviano*, pp. 161–169, Santa Cruz de la Sierra, 1994.

Besse, J., and V. Courtillot, Revised and synthetic apparent polar wander paths of the African, Eurasian, North American and Indian plates, and true polar wander since 200 Ma, *J. Geophys. Res.*, 96, 4029–4050, 1991.

Briden, J. C., Paleozoic a.p.w. paths and continental reassemblies: A case of faltering progress (abstract), *Eos Trans. AGU*, *73*(14), Spring Meet. Suppl., 51, 1992.

Butler, R. F., D. R. Richards, T. Sempere, and L. G. Marshall, Paleomagnetic determinations of vertical-axis tectonic rotations from Late Cretaceous and Paleocene strata of Bolivia, *Geology*, *23*, 799–802, 1995.

Creer, K. M., A palaeomagnetic survey of South American rock formations, *Philos. Trans. R. Soc. London, Ser. A.*, *267*, 457–558, 1970.

Dunlop, D. J., Magnetic mineralogy of unheated and heated red sediments by coercivity spectrum analysis, *Geophys. J. R. Astron. Soc.*, *27*, 37–55, 1972.

Ernesto, M., L. A. Diogo, and A. C. Rocha-Campos, Paleomagnetism of the Subandean Carboniferous ("Gondwana") sequence in Bolivia: Tectonic implications, in *Gondwana Seven*, edited by H. Ulbrich and A. C. Rocha-Campos, pp. 615–636, Sao Paulo, Brazil, 1988.

Fisher, R. A., Dispersion on a sphere, *Proc. R.. Soc. London, Ser. A*, 217, 295–305, 1953.

Garven, G., and R. A. Freeze, Theoretical analysis of the role of groundwater flow in the genesis of stratabound ore deposits, *Am. J. Sci.*, *284*, 1125–1174, 1984.

Graham, J. W., The stability and significance of magnetism in sedimentary rocks, *J. Geophys. Res.*, *54*, 131–167, 1949.

Hargraves, R. B., E. M. Dawson, and F. B. Van Houten, Palaeomagnetism and age of mid-Palaeozoic ring complexes in Niger, West Africa, and tectonic implications, *Geophys. J. R. Astron. Soc.*, *90*, 705–729, 1987.

Hartley, A. J., E.J. Jolley, and P. Turner, Paleomagnetic evidence for rotation in the Precordillera of northern Chile: Structural constraints and implications for the evolution of the Andean forearc, *Tectonophysics*, *205*, 49–64, 1992.

Hurley, N. F., and R. Van der Voo, Paleomagnetism of Upper Devonian reefal limestones, Canning basin, western Australia, *Geol. Soc. Am. Bull.*, *98*, 138–146, 1987.

Irving, E., and G. A. Irving, Apparent polar wander paths Carboniferous through Cenozoic and the assembly of Gondwana, *Geophys. Surv.*, *5*, 141–188, 1982.

Kirschvink, J. L., The least-squares line and plane and the analysis of palaeomagnetic data, *Geophys. J. R. Astron. Soc.*, *62*, 699–718, 1980.

Lawrence, S. R., and C. Cornford, Basin geofluids, *Basin Res.*, *7*, 1–7, 1995.

Lowrie, W., Identification of ferromagnetic minerals in a rock by coercivity and unblocking temperature properties, *Geophys. Res. Lett.*, *17*, 159–162, 1990.

McCabe, C., and R. D. Elmore, The occurrence and origin of Late Paleozoic remagnetization in the sedimentary rocks of North America, *Rev. Geophys.*, *27*, 471–494, 1989.

McFadden, P. L., A new fold test for palaeomagnetic studies, *Geophys. J. Int.*, *103*, 163–169, 1990.

McFadden, P. L., and A. B Reid, Analysis of palaeomagnetic inclination data, *Geophys. J. R. Astron. Soc.*, *69*, 307–319, 1982.

Oliver, J., Fluids expelled tectonically from orogenic belts: Their role in hydrocarbon migration and other geologic phenomena, *Geology*, *14*, 99–102, 1986.

Randall, D. E., G. K. Taylor, and J. Grocott, Major crustal rotations in the Andean margin: Paleomagnetic results from the Coastal Cordillera of northern Chile, *J. Geophys. Res.*, *101*(B7), 15,783–15,798, 1996.

Raposo, M., and M. Ernesto, An Early Cretaceous paleomagnetic pole from Ponta Grossa dikes (Brazil): Implications for the South American Mesozoic apparent polar wander path, *J. Geophys. Res.*, *100*(B10), 20,095–20,109, 1995.

Roperch, P., and G. Carlier, Paleomagnetism of Mesozoic rocks from the Central Andes of Southern Peru: Importance of rotations in the development of the Bolivian orocline, *J. Geophys. Res.*, *97*(B12), 17,233–17,249, 1992.

Scotese, C. R., R. Van der Voo, and C. McCabe, Paleomagnetism of the Upper Silurian and Lower Devonian carbonates of New York State: Evidence for secondary magnetization residing in magnetite, *Phys. Earth Planet. Inter.*, *30*, 385–395, 1983.

Sempere, T., Phanerozoic evolution of Bolivia and adjacent regions, in *Petroleum Basins of South America*, edited by A. J. Tankard, R. Suarez, and H. J. Welsink, *AAPG Mem.*, *62*, 207–230, 1995.

Sempere, T., G. Hérail, J. Oller, and M. G. Bonhomme, Late Oligocene–early Miocene major tectonic crisis and related basins in Bolivia, *Geology*, *18*, 946–949, 1990.

Sempere, T., E. Aguilera, J. Doubinger, P. Janvier, J. Lobo, J. Oller, and S. Wenz, La Formation de Vitiacua (Permien moyen a superieur-Trias ?inferieur, Bolivia de Sud); stratigraphie, palynologie et paleontologie, *Neues Jahrb. fuer Geol. Palaeontol. Abh.*, *185*(2), 239–253, 1992.

Sempere, T., R. F. Butler, D. R. Richards, L. G. Marshall, W. Sharp, and C. C. Swisher III, Stratigraphy and geochronology of Upper Cretaceous–lower Paleogene strata in Bolivia and northwest Argentina, *Geol. Soc. Am. Bull.*, *109*, 709–727, 1997.

Stamatakos, J., A. M. Hirt, and W. Lowrie, The age and timing of folding in the central Appalachians from paleomagnetic results, *Geol. Soc. Am. Bull., 108*, 815–829, 1996.

Van der Voo, R., Paleozoic paleogeography of North America, Gondwana, and intervening displaced terranes: Comparisons of paleomagnetism with paleoclimatology and biogeographical patterns, *Geol. Soc. Am. Bull., 100*, 311–324, 1988.

Watson, G. S., A test for randomness of directions, *Mon. Not. Geophys. J. R. Astron. Soc., 7*, 160–161, 1956.

Watson, G. S., and E. Irving, Statistical methods in rock magnetism, *Mon. Not. Geophys. J. R. Astron. Soc., 7*, 289–300, 1957.

R. F. Butler, J. C. Libarkin, and D. R. Richards, Department of Geosciences, University of Arizona, Tucson, AZ 85721. (e-mail: libarkin@geo.arizona.edu)

T. Sempere, Misión Orstom en el Perú, Casilla 18–1209, Lima 18, Perú.

(Received March 12, 1998; revised July 15, 1998;
accepted August 24, 1998.)